April 2004

Formations of Localization of Robot Networks

Fan Zhang
University of Pennsylvania, zhangfan@grasp.cis.upenn.edu

Ben Grocholsky
University of Pennsylvania, bpg@grasp.cis.upenn.edu

R. Vijay Kumar
University of Pennsylvania, kumar@grasp.upenn.edu

Copyright 2004 IEEE. Reprinted from *Proceedings of the IEEE International Conference on Robotics and Automation 2004 (ICRA 2004)* Volume 4, pages 3369-3374.
Publisher URL: http://ieeexplore.ieee.org/xpl/tocresult.jsp?isNumber=29027&page=2

Formations of Localization of Robot Networks

Abstract
In this paper, we consider the problem of cooperatively localizing a formation of networked mobile robots/vehicles in SE(2), and adapting the formation to reduce localization errors. First, we propose necessary and sufficient conditions to establish when a team of robots with heterogeneous sensors can be completely localized. We present experimental measurements of range and bearing with omni-directional cameras to motivate a simple model for noisy sensory information. We propose a measure of quality of team localization, and show how this measure directly depends on a *sensing graph*. Finally, we show how the formation and the sensing graph can be adapted to improve the measure of performance for team localization and for localization of targets through experiments and simulations.

Proceedings of the 2004 IEEE
International Conference on Robotics & Automation
New Orleans, LA • April 2004

Formations for Localization of Robot Networks

Fan Zhang Ben Grocholsky Vijay Kumar
GRASP Laboratory, University of Pennsylvania, Philadelphia, PA 19104, USA
{zhangfan, bpg, kumar}@grasp.cis.upenn.edu

Abstract— **In this paper, we consider the problem of cooperatively localizing a formation of networked mobile robots/vehicles in $\mathbb{SE}(2)$, and adapting the formation to reduce localization errors. First, we propose necessary and sufficient conditions to establish when a team of robots with heterogeneous sensors can be completely localized. We present experimental measurements of range and bearing with omni-directional cameras to motivate a simple model for noisy sensory information. We propose a measure of quality of team localization, and show how this measure directly depends on a *sensing graph*. Finally we show how the formation and the sensing graph can be adapted to improve the measure of performance for team localization and for localization of targets through experiments and simulations.**

I. Introduction

In order for a team of mobile robots to navigate autonomously in some desired formations and further perform cooperative tasks, such as surveillance and target acquisition, they must be able to localize themselves in the formation as well as in a global reference frame [1], [2]. Therefore, how to estimate robots' positions and orientations (poses) in a precise and efficient way is of particular interest. Our interest in this paper is localizing a team of heterogeneous robots in $\mathbb{SE}(2)$, and in localizing targets with information obtained from heterogeneous sensors. Specifically, we are interested in conditions under which all robots in the formation can be localized in the environment, and in minimizing the relative and absolute uncertainty in the estimates. Our goal in this paper is to derive necessary and sufficient conditions for localizing a formation of three or more robots in $\mathbb{SE}(2)$ from distributed camera measurements, quantifying the quality of the resulting estimates, and adapting the team formation to improving these estimates.

Recent research has addressed the problem of network localization in non-deterministic domains. Examples of fusing observations from heterogeneous sensors to estimate the state of a robot team include the distributed Kalman filter [3] and maximum likelihood [4] methods. These approaches consider communication and computational cost but do not address the impact of robot formation on the quality of the solution obtained. Other studies investigate generating optimal sensing trajectories for robots engaged in target tracking tasks given the robot state is known exactly [5], [6]. The work presented in this paper addresses the combination of these two problems. Given the fact that the quality of estimates obtained from measurements depends on how well sensors can be localized, we extend these ideas to find an optimal formation control scheme which will facilitate not only maximal target localization but also consider the robot configuration estimate quality.

Also relevant to this work is the recent literature that uses graphs to model sensor networks and cooperative control schemes [7], [8]. Results on graph rigidity theory [9], [10], [11] can be directly applied to multi-robot systems in $\mathbb{R}^2$ [12], [13]. However, relatively little attention has been paid on networks with bearing observations, which is particularly important for networks of cameras.

This paper is organized as follows. In Section II, formations of mobile robots and sensor measurement information will be modeled topologically via graph theory notations. Without considering measurement error at first, we generate the concepts of formation constraint and constraint matrix in Section III, and use them to find the necessary and sufficient conditions for a formation to be localizable. Measurement errors and their connection to estimate errors are introduced in Section IV, and the dependence of localization quality on the sensing graph and formation geometry is also investigated. A control strategy for determining optimal formations is presented. Practical application of these concepts to a small team of robots equipped with omni-directional cameras follows in Section V. The camera modelling, performance impact of the sensing graph and robot deployment to an optimal configuration are detailed. Concluding remarks are given in Section VI.

II. Modeling

Consider a planar world, $\mathcal{W} = \mathbb{R}^2$, occupied by a team of n robots, $\mathcal{R} = \{R_1, R_2, \ldots R_n\}$, and assume each robot can communicate with every other robot in the team. The physical configurations of the robots coupled with the characteristics of the hardware and the requirements of the sensing and control algorithms induce a *physical network* or a *formation* of n robots in $\mathbb{SE}(2)$. We define a global reference frame $\mathcal{F}$ by forming a virtual robot or a beacon R_0 with fixed configuration

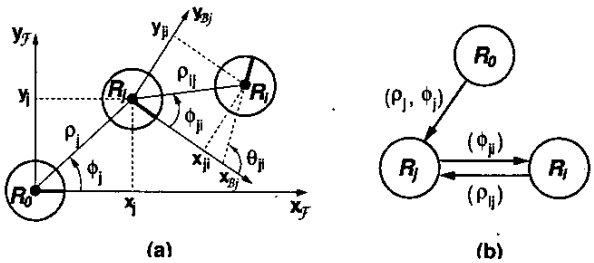

Fig. 1. Modeling of sensory information: (a) - physical network of 2 robots in $\mathbb{SE}(2)$: R_i has range measurements about R_j; R_j has absolute measurements about itself and bearing measurements about R_i. A body reference frame, $\mathcal{B}_j$, has been attached to R_j. (b) - sensing graph representation.

$q_0 = 0$ in the inertial frame. (See Figure 1(a)). The configuration of $\mathcal{R}$ in $\mathcal{F}$ is denoted by $\bar{q} = \left[q_1^T, q_2^T, \ldots, q_n^T\right]^T \in \mathbb{R}^{3n}$, where $q_i = (p_i, \theta_i)^T \in \mathbb{R}^3$ is a parameterization of $\mathbb{SE}(2)$, with $p_i = (x_i, y_i)^T$ and θ_i, the absolute position and orientation of the i^{th} robot. A body reference frame $\mathcal{B}_j$ at the j^{th} robot is also defined with its x-axis aligned with the direction of heading of R_j. The configuration or the *shape* of the formation, $\mathcal{R}$, is described in the body-fixed frame $\mathcal{B}_j$ by $\tilde{q} = [(q_1^j)^T, (q_2^j)^T, \ldots, (q_n^j)^T]^T$, where $q_i^j = (p_{ji}, \theta_{ji})^T$ with $p_{ji} = (x_{ji}, y_{ji})^T$ and θ_{ji}, the relative position and orientation of R_i about R_j, and $q_j^j = 0$.

In [7], [2], we defined the *control graph*, a directed graph in which each edge represents an interconnection linking the control inputs of one robot to the state of another. Here, in order to represent the sensory information, we define another directed graph called the *sensing graph*, $\mathcal{G} = (\mathcal{V}, \mathcal{E}, \mathcal{Z}, \mathcal{P})$, where $\mathcal{V} = \mathcal{R} \cup \{R_0\}$ is a finite set of vertices. The edge set $\mathcal{E} \subset \mathcal{V} \times \mathcal{V}$ consists of labeled edges that represent the presence of measurements (observations) between robots. We consider three types of exteroceptive sensors: range sensors, bearing sensors, and GPS sensors. The measurement set $\mathcal{Z}$ consists of three type of sensory information: (i) range between two robots, ρ_{ij}, (ii) bearing of one robot in relation to another, ϕ_{ij}, and (iii) absolute position of a robot in $\mathcal{F}$, (x_j, y_j), which can be obtained by global positioning sensors, or via triangulation with fixed, known landmarks. $\mathcal{P}$ is a model of the uncertainties associated with the estimates in $\mathcal{Z}$.

In a sensing graph $\mathcal{G}$, the j^{th} vertex has an incoming edge from the i^{th} vertex labeled by (ρ_{ij}, ϕ_{ij}) whenever robot R_i can sense robot R_j. Corresponding to types of sensory information, we use (i) a shorthand *relative range edge* (ρ_{ij}) to denote $(\rho_{ij}, null)$, (ii) a *relative bearing edge* (ϕ_{ij}) for $(null, \phi_{ij})$ and (iii) a *range-bearing edge* (ρ_{ij}, ϕ_{ij}) pointed from R_i to R_j respectively. Any absolute measurements made by any robot R_j can be regarded as a range-bearing edge, (ρ_{j0}, ϕ_{j0}), or simply (ρ_j, ϕ_j).

In the next section we will consider a deterministic setting to determine necessary and sufficient conditions on the sensing graph for team localization. We will later, in Section IV, consider uncertainties in measurements, with $\mathcal{P}$ consisting of information about variances: $\sigma^2_{\rho_{ij}}$ for range measurements, $\sigma^2_{\phi_{ij}}$ for bearing measurements, and covariance matrices for range-bearing measurements.

III. Localizability of Formations

In order to consider whether a team of robots can be localized or not, it is necessary to fuse the information available from different sensors and verify if this information is adequate. For a team of n robots in $\mathbb{SE}(2)$, localization is the determination of the $3n$ coordinates that characterize the robot positions and orientations. Thus it is necessary to first see if $3n$ independent measurements are available or not. Since every measurement specifies a constraint on the $3n$ coordinates, we have to develop a test of functional independence for all constraints. Accordingly, we will define a *constraint matrix* whose rank will allow us to verify if the team can be localized or not.

For each range and bearing measurement, the constraints on the coordinates in frame $\mathcal{B}_j$ are given by:

$$Type\ 1:\ \rho_{ik} = \sqrt{(p_{ji} - p_{jk})^T (p_{ji} - p_{jk})} \tag{1}$$

$$Type\ 2:\ \phi_{ji} = tan^{-1}(y_{ji}/x_{ji}) \tag{2}$$

A pair of bearing measurements, ϕ_{ij} and ϕ_{ji}, involving robots R_i and R_j, results in the following Type 3 constraint:

$$Type\ 3:\ \phi_{ik} - \phi_{ki} + \pi = \theta_{ik} = \theta_{jk} - \theta_{ji} \tag{3}$$

Finally, any pair of bearing measurements, ϕ_{ij} and ϕ_{jk}, involving three robots R_i, R_j, and R_k, results in the following Type 4 constraint.

$$Type\ 4:\ \phi_{ij} - \phi_{ik} = cos^{-1} \frac{(p_{ji} - p_{jj})^T (p_{ji} - p_{jk})}{\|p_{ji} - p_{jj}\| \cdot \|p_{ji} - p_{jk}\|} \tag{4}$$

All these constraints can be written in the form:

$$L_1 \cdot z = h(\tilde{q}) \tag{5}$$

where L_1 is a linear combination of measurements, and h is a nonlinear function of the shape variables in some body-fixed reference frame. It is not too difficult to see that there are only four types of constraints that can be used to describe the network. All other equations that can be written are functionally dependent on the above constraint equations.

By differentiating the four constraint equations, we get expressions describing allowable small changes (equivalently velocities) of the robot coordinates.

$$\begin{bmatrix} r_{1,ik} & r_{2,ik} \end{bmatrix} \begin{bmatrix} \dot{p}_{ji} \\ \dot{p}_{jk} \end{bmatrix} = 0 \tag{6}$$

$$\begin{bmatrix} \frac{-y_{ji}}{p_{ji}^T p_{ji}} & \frac{x_{ji}}{p_{ji}^T p_{ji}} \end{bmatrix} \begin{bmatrix} \dot{p}_{ji} \end{bmatrix} = 0 \tag{7}$$

$$\begin{bmatrix} -1 & 1 \end{bmatrix} \begin{bmatrix} \dot{\theta}_{ji} \\ \dot{\theta}_{jk} \end{bmatrix} = 0 \tag{8}$$

$$\begin{bmatrix} b_{1,jik} & b_{2,jik} & b_{3,jik} \end{bmatrix} \begin{bmatrix} \dot{p}_{ji} \\ \dot{p}_{jj} \\ \dot{p}_{jk} \end{bmatrix} = 0 \tag{9}$$

where

$$r_{1,ik} = \frac{p_{ji} - p_{jk}}{\sqrt{(p_{ji} - p_{jk})^T (p_{ji} - p_{jk})}} \quad r_{2,ik} = \frac{p_{jk} - p_{ji}}{\sqrt{(p_{ji} - p_{jk})^T (p_{ji} - p_{jk})}}$$

$$b_{1,jik} = \frac{2[(p_{ji} - p_{jj})^T (p_{ji} - p_{jk})]}{(p_{ji} - p_{jj})^2 (p_{ji} - p_{jk})^2} (2p_{ji} - p_{jj} - p_{jk}) - \frac{2[(p_{ji} - p_{jj})^T (p_{ji} - p_{jk})]^2}{(p_{ji} - p_{jj})^4 (p_{ji} - p_{jk})^2} (p_{ji} - p_{jj}) - \frac{2[(p_{ji} - p_{jj})^T (p_{ji} - p_{jk})]^2}{(p_{ji} - p_{jj})^2 (p_{ji} - p_{jk})^4} (p_{ji} - p_{jk})$$

$$b_{2,jik} = \frac{2[(p_{ji} - p_{jj})^T (p_{ji} - p_{jk})]}{(p_{ji} - p_{jj})^2 (p_{ji} - p_{jk})^2} (p_{jk} - p_{ji}) + \frac{2[(p_{ji} - p_{jj})^T (p_{ji} - p_{jk})]^2}{(p_{ji} - p_{jj})^4 (p_{ji} - p_{jk})^2} (p_{ji} - p_{jj})$$

$$b_{3,jik} = \frac{2[(p_{ji} - p_{jj})^T (p_{ji} - p_{jk})]}{(p_{ji} - p_{jj})^2 (p_{ji} - p_{jk})^2} (p_{jj} - p_{ji}) \quad \ldots$$

$$+\frac{2[(p_{ji}-p_{jj})^T(p_{ji}-p_{jk})]^2}{(p_{ji}-p_{jj})^2(p_{ji}-p_{jk})^4}(p_{ji}-p_{jk})$$

Following this procedure for all possible constraints gives us a $m \times 3n$ constraint matrix for reference frame $\mathcal{B}_j$:

$$K_f(\tilde{q})\ \dot{\tilde{q}} = 0 \tag{10}$$

where

$$K_f = \begin{bmatrix} \cdot\cdot & r_{1,ik} & \cdot\cdot & r_{2,ik} & \cdot\cdot & \cdot\cdot & \cdot\cdot \\ \cdot\cdot & (\frac{-y_{ji}}{p_{ji}^T p_{ji}}\ \frac{x_{ji}}{p_{ji}^T p_{ji}}) & \cdot\cdot & \cdot\cdot & \cdot\cdot & \cdot\cdot & \cdot\cdot \\ \cdot\cdot & \cdot\cdot & -1 & \cdot\cdot & 1 & \cdot\cdot & \cdot\cdot \\ \cdot\cdot & b_{1,jik} & \cdot\cdot & b_{2,jik} & \cdot\cdot & b_{3,jik} & \cdot\cdot \\ \vdots & \vdots & \vdots & \vdots & \vdots & \vdots & \vdots \end{bmatrix}$$

$K_f = \frac{\partial h}{\partial \tilde{q}_j}$ is called the *constraint matrix* for the formation.

Definition 1: A team of n robots in $\mathbb{SE}(2)$ is said to be *localizable* if the $3n$ coordinates of the n robots can be estimated in an inertial frame.

Remark 1: Localizability is obviously related to observability in systems theory [14] – if a team is localalizable over any time interval, the system is completely observable. However, we will use Definition 1 in an instantaneous, static setting and thus refrain from using systems theoretic notation.

Remark 2: We can also require the team to be localized in a relative setting [2] where it is only necessary to able to estimate $3n-3$ coordinates of $n-1$ robots in a body reference frame.

Theorem 1: A formation of n robots in $\mathbb{SE}(2)$ is localizable only if

$$N = 3n - 2n_g - n_b - n_r \leq 0, \tag{11}$$

where n_g, n_b and n_r are numbers of measurements made by inertial or global positioning sensors, bearing sensors and range sensors respectively.

Proof: It is easy to verify that each absolute position measurement made by any global positioning sensor can be directly used to estimate two state variables, and each bearing and range measurement will add at least one constraint on the configuration or shape of the formation. Thus, n_g global position sensors, n_b bearing sensors and n_r range sensors will provide at most $2n_g + n_b + n_r$ independent measurements. Since $3n$ state variables have to be estimated, $2n_g + n_b + n_r$ must be at least equal to $3n$. ■

Given a formation of robots with limited sensing capability, Theorem 1 provides a simple necessary condition to easily verify the localizability without considering the formation geometry. Note that additional sensors such as landmark sensors, compasses and IMUs can be incorporated into this framework in a straightforward way. The following discussion provides sufficient conditions for localizability.

Theorem 2: Consider a formation of n robots in $\mathbb{SE}(2)$ with the shape $\tilde{q} = [(q_1^j)^T, (q_2^j)^T, \ldots, (q_n^j)^T]^T$ in $\mathcal{B}_j$. The formation is localizable relative to the robot-fixed reference frame $\mathcal{B}_j$ if and only if

$$rank\{K_f(\tilde{q})\} = 3n - 3,\ (n \geq 2). \tag{12}$$

Proof: Any body-fixed description of a formation in $\mathbb{SE}(2)$ has a natural group symmetry. Translation of this body-fixed reference frame does not change the shape vector $\tilde{q} = [(q_1^j)^T, (q_2^j)^T, \ldots, (q_n^j)^T]^T \in \mathbb{R}^{3n}$. Thus there are $3n-3$ free variables that determine the shape of the formation in the frame $\mathcal{B}_j$. Since the rank of K_f determines the number of independent constraints imposed by sensor measurements in the network, we must have:

$$rank\{K_f\} = 3n - 3$$

in order to estimate the $3n-3$ nonzero variables in $\tilde{q}$. ■

The condition in Theorem 1 is only a weak necessary condition. There are other necessary conditions that must be satisfied. We are particularly interested in cases where global positioning capability is not available to most robots. For example, if $n_g = 0$ or 1, it follows from Theorem 2 that we need at least one range measurement leading to a Type 1 constraint and $n-1$ pairs of bearing measurements leading to Type 3 constraints. At least one Type 2 constraint must be incorporated. And finally, for localization in an inertial frame, one needs at least one global position estimate ($n_g > 0$), and at least one bearing measurement of the virtual robot (*i.e.*, a measurement ϕ_{j0}).

IV. Dependence of Estimation Errors on Sensing Graph and Formation Geometry

In this section we assume a simple probabilistic model for sensor measurements and show how errors in state estimates depend on (a) the sensing graph, $\mathcal{G}$; and (b) the shape of the formation. In order to keep the analysis simple, we will assume that the measurement noise is given by a joint normal distribution. As shown later in Section V-A, our range sensor measurements are normally distributed and it is reasonable to assume that sensory measurements are independent. Accordingly, the constraint equation in Equation 5 can be rewritten as:

$$L_1 \cdot z = h(\tilde{q}) + L_2 \cdot \nu_0 \tag{13}$$

where z is the vector of measurements, $\tilde{q}$ is the shape of the formation in $\mathcal{B}_j$, $\nu_0 \sim N(0, R_0)$ is the vector of measurements' noise (assuming zero-mean independent noise and hence a diagonal covariance matrix R_0), and $h(\tilde{q})$ represents the nonlinearity in the constraints, Equations 1-4. L_i are matrices representing constant linear combinations of z and ν_0. For example, if we consider Equation 3, the standard deviations, $\sigma_{\phi_{ij}}$, $\sigma_{\phi_{ji}}$, and $\sigma_{\theta_{ij}}$ satisfy

$$\sigma_{\phi_{ij}}^2 + \sigma_{\phi_{ji}}^2 = \sigma_{\theta_{ij}}^2$$

and thus

$$L_1 = [\,-1 \quad 1\,] \qquad L_2 = [\,1 \qquad 1\,]$$

If we define ν to be the vector given by $\nu = L_2 \cdot \nu_0$, ν is also normally distributed with the expected value 0, and the variance given by:

$$R = L_2\ R_0\ L_2^T \tag{14}$$

Thus $\nu \sim N(0, R)$ characterizes the noise in Equation 13.

In order to obtain the best estimate for the formation shape, $\tilde{q}$, we can use a nonlinear least squares algorithm to solve Equation 13. Clearly, the total number of constraint equations, m, must be at least $3n-3$, but at most equal to the number of measurements, M. Thus,

$$3n-3 \leq m \leq M, \ (n \geq 2) \tag{15}$$

Now let H be a $m \times (3n-3)$ matrix obtained by deleting the three columns corresponding to the jth robot's coordinates q_j^j in K_f. Let x_j be the $3n-3$ vector obtained by deleting the three variables corresponding to q_j^j in $\tilde{q}$. Small changes in x_j denoted by δx_j will be related to small changes in z, denoted by δz, according to:

$$L_1 \delta z = H \delta x \tag{16}$$

Minimizing the weighted cost $(L_1\delta z - H\delta x)^T W (L_1 \delta z - H \delta x)$ leads to [14]

$$\delta x = (H^T W H)^{-1} H^T W L_1 \delta z \tag{17}$$

Setting the weighting matrix $W = R^{-1}$, squaring equation (17) by multiplying both sides of the equation by their transposes respectively and then taking the expectations on both sides, we can get the covariance matrix P for errors of coordinate estimates as

$$P = (H^T W H)^{-1} H^T W R W^T H (H^T W H)^{-T}$$

or simply

$$P = (H^T R^{-1} H)^{-1} \tag{18}$$

Obviously, the localization errors are affected by the specific set of measurements and corresponding constraint equations we use. Additionally, the terms of the constraint matrix observed in Sections III indicate the estimate error covariance resulting from Equation 18 depends on the robot spatial configuration. The trace of the covariance matrix is a scalar utility measure that captures quality of the estimate obtained from a measurement set. This leads to a natural strategy for comparison and optimization of sensing graphs and robot formations for localization. The robot configuration is sought that for a given a sensor assignment solves

$$p = \arg \min_{p \in \mathcal{W}} \text{trace} P. \tag{19}$$

Gradient descent provides a mechanism to drive sensing elements to the optimal spatial configuration. Controlling robot velocity according to

$$\dot{p} = -k \frac{\partial}{\partial p} \text{trace}(P) \tag{20}$$

yields trajectories that realize the desired formation.

Using the matrix calculus relations

$$\frac{\partial}{\partial x}\text{trace}(X) = \text{trace}(\frac{\partial}{\partial x} X) \text{ and } \frac{\partial}{\partial x} X = -X \frac{\partial}{\partial x}(X^{-1}) X,$$

The control strategy, Equation 20 can be written directly in terms of $\frac{\partial}{\partial p} H$ (available analytically) as

$$\dot{p} = -k \text{ trace} \left[-P \left(\frac{\partial}{\partial p} H^T R^{-1} H + H^T R^{-1} \frac{\partial}{\partial p} H \right) P \right]. \tag{21}$$

V. Results in Robot Localization and Active Sensing Network Deployment

The concepts developed in this paper are applied to a small robot team. Three examples are presented to illustrate the physical sensor characteristics, implications of the sensing graph on localization performance and active robot deployment to maximize team localization performance.

A. Omni-Directional Camera Model Verification

The omni-directional camera detailed in Figure 2 utilizes a parabolic mirror in order to enable a single camera to directly measure both range and bearing to a feature. The mirror

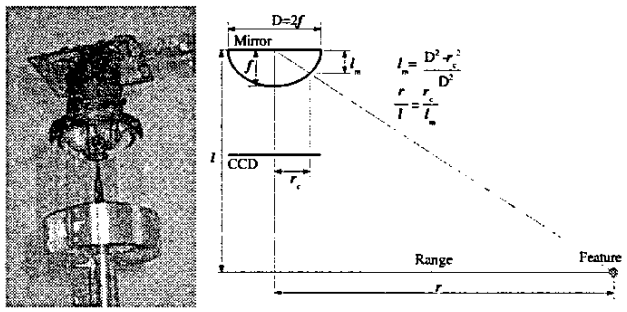

Fig. 2. Parabolic Omni-directional Camera and Geometry

geometry introduces a nonlinear observation model that relates measurements $z = r_c$ to the feature state (range) $x = r$, given by

$$z = h(x) + \nu = \frac{D}{x}\left(\sqrt{l^2 + x^2} - l\right) + \nu. \tag{22}$$

Where ν in measurement noise $p(\nu) \sim \mathcal{N}(0, R)$. For signal levels where linearization is valid, noise in observations of $\mathbf{x}$ derived from measurements $\mathbf{z}$, will be the measurement noise amplified by $(H^T R^{-1} H)^{-1}$. For the model described by Equation 22,

$$H = \frac{\partial h}{\partial x} = \frac{x^2 \sqrt{l^2 + x^2}}{Dl\left(\sqrt{l^2 + x^2} - l\right)} \tag{23}$$

This indicates the variance of range observations obtained from the omni-directional camera is approximately proportional to the fourth power of the true feature range.

Experiments were conducted to validate use of this modelling. The camera was rotated about its vertical axis while observing a static feature at various known ranges. Measurements of feature centroid in the camera coordinates and a histogram of corresponding range observations are shown in Figure 3. Figure 4 compares the range observation standard deviation observed experimentally to parabolic omni-directional camera model, verifying the predicted range dependent measurement uncertainty.

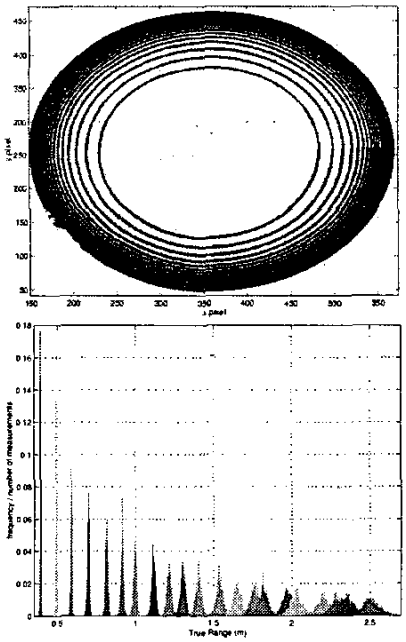

Fig. 3. Omni-Directional camera measurements and feature range histogram

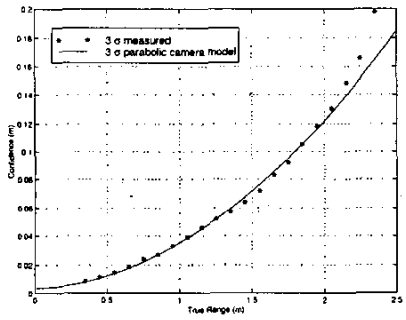

Fig. 4. Measured and modeled range measurement uncertainty

B. Multi-Robot Localization Experiments

To investigate the dependence of estimation errors on sensing graph as we discussed in Section IV, localization experiments on a team of 5 car-like mobile robots equipped with omni-directional cameras (see Figure 5) were conducted. In the experiments, the robot team maintained a static formation on the ground, and tried to localize each member in the formation by taking relative measurements with respect to each other. In order to simplify visual classification and association, each robot was marked with a different color providing unique sensor identification for each robot. A calibrated overhead camera with an external computer was used to gather the ground true data for the robot locations in the environment.

While all the necessary and sufficient conditions for team localization provided in Section III are strictly maintained, there still exist extra degrees of freedom in choosing the measurement set and corresponding constraint equations to achieve the

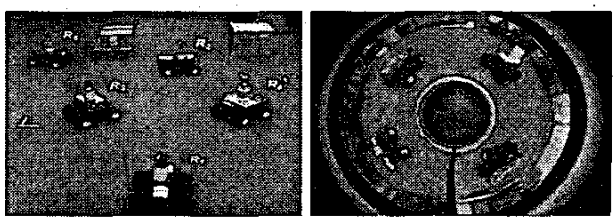

Fig. 5. A formation of five car-like mobile robots (left) and a sample image from omni-directional camera (right).

estimation. As an example, six sets of measurements, which are denoted by six sensing graphs in Figure 6, were used to estimate the state of five robots in the experiment respectively. Equation 18 was applied to compute the covariance matrix of estimation errors for each sensing graph considered. Table I shows the corresponding localization quality, quantified by the trace of the error covariance matrix.

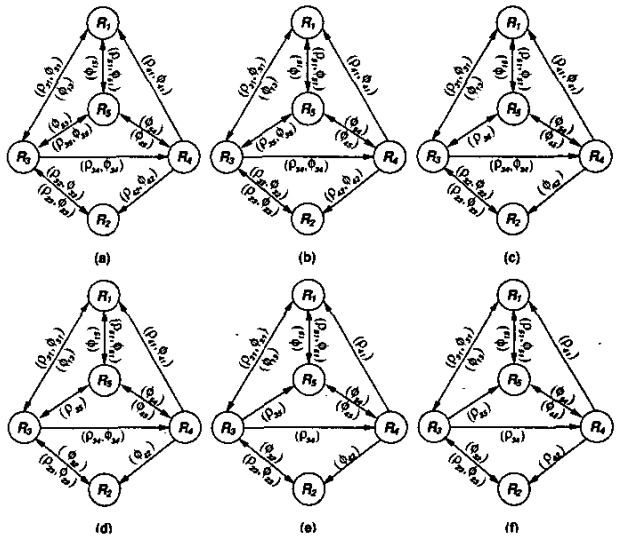

Fig. 6. Sensing Graphs used to illustrate impact on localization quality. (a) - contains all available measurements. (b) - contains all measurements except for ϕ_{53}. (c) - case b with ϕ_{35} and ρ_{42} removed. (d) - case c with ρ_{32} removed. (e) - contains the graph that maximizes estimate quality subject to using the minimum number of measurements required for localizability. (f) - as in case e with one bearing measurement ϕ_{42} substituted by ρ_{42}.

TABLE I
ESTIMATE QUALITY FOR DIFFERENT SENSING GRAPHS

	Case a	Case b	Case c	Case d	Case e	Case f
Trace	0.0142	0.0142	0.0171	0.0228	0.1231	0.1505

As expected, Table I indicates that the localization quality was improved when more measurement information was used to construct the sensing graph. However, comparing the cases provides insight to the process of sensing graph selection. The removal of ϕ_{53} in case b does not significantly reduce localization quality. This indicates ϕ_{53} is relatively uninforma-

tive given the measurements in graph b. Considering the cost of processing additional measurements motivates selecting a measurement sub-graph when redundancy is high.

Substitution of a bearing measurement for range measurement improves the estimate quality obtained in case e over f. This outcome is expected considering the characteristics of the omni-directional camera, the other measurements used and the true shape of the robot formation. However, impact of an individual measurement can not be determined independently of other graph assignments. Solutions to this difficult nonlinear assignment are of significant practical interest.

C. Optimal Formation Deployment

In this case (see Figure 7), three mobile robots are deployed to collaboratively localize themselves and a target of interest in R_0's reference frame. A minimum number of relative measurements are used to achieve localization. The initial compact formation of R_1, R_2 and R_3 close to R_0 yields poor target localization degrading overall localization performance. The control scheme described by Equation 21 is applied to improve this situation. Each robot moves along a trajectory governed by the gradient of the trace of the error covariance matrix. The configuration of this mobile sensor network converges to an optimal formation, where the quality of overall team location estimation is maximized.

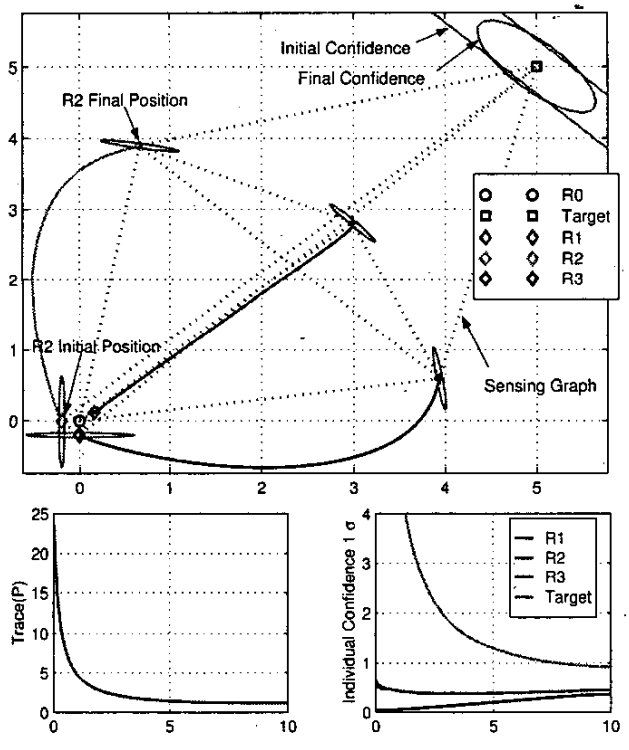

Fig. 7. Three mobile robots/sensors deploy to collectively localize themselves and a target of interest using a minimal sensing graph containing the relative measurements $z = \{\phi_{01}, \rho_{10}, \rho_{12}, \rho_{13}, \rho_{20}, \rho_{23}, \rho_{2T}, \rho_{30}, \rho_{3T}\}$. Where ρ_{iT} denotes the relative range measurement between the i_{th} robot and the target.

VI. Conclusions

In this paper, we presented a graphical model of robot-sensor networks in $\mathbb{SE}(2)$, and derived the sufficient and necessary conditions for building rigid sensing graphs and localizable formations based on distributed exteroceptive sensors. The affect of the sensing graphs and the robot formation geometry on localization quality was investigated using experimentally validated sensor modelling. A gradient based control scheme was applied to deploy robot teams to configurations that maximize the quality of localization estimates obtained.

VII. Acknowledgements

This work was in part supported by: DARPA MARS NBCH1020012, ARO MURI DAAD19-02-01-0383, and NSF CCR02-05336. The authors would like acknowledge the valuable advice from Prof. Max Mintz and the experiment development effort of Guilherme Pereira.

References

[1] C. Belta and V. Kumar, "Motion generation for formation of robots: a geometric approach," in *Proceedings of International Conference on Robotics and Automation, Seoul, Korea*, 2001.

[2] A. Das, J. Spletzer, , V. Kumar, and C. Taylor, "Ad hoc networks for localization and control," in *Proceedings of the 41st IEEE Conference on Decision and Control, Las Vegas, NV*, 2002.

[3] S. Roumeliotis and G. Bekey, "Collective localization: a distributed kalman filter approach to localization of groups of mobile robots," in *Proceedings of the IEEE International Conference on Robotics and Automation, San Francisco, California*, 2000, pp. 2958–2965.

[4] A. Howard, M. Matari, and C. Sukhatme, "Team localization: a maximum likelihood approach," in *Technical Report IRIS-01-415, Institute for Robotics and Intelligent Systems Technical Report, University of Sourthern California*, 2002.

[5] J. Spletzer and C. Taylor, "Dynamic sensor planning and control for optimally tracking targets," *International Journal of Robotics Research*, vol. 22, pp. 7–20, 2003.

[6] B. Grocholsky, A. Makarenko, T. Kaupp, and H. Durrant-Whyte, "Scalable control of decentralised sensor platforms," in *Information Processing in Sensor Networks: 2nd Int Workshop, IPSN03*, 2003, pp. 96–112.

[7] A. Desai, V. Kumar, and J. Ostrowski, "A theoretical framework for modeling and controlling formation of mobile robot," *IEEE Transactions on Robotics and Automations*, 2001.

[8] G. Pappas, P. Tabuada, and P. Lima, "Feasible formations of multi-agent systems," in *Proceedings of the American Control Conference, Arlington, Virginia*, 2001.

[9] G. Laman, "On graphs and rigidity of plane skeletal structures," *Journal of Engineering Mathematics*, vol. 4, pp. 331–340, October 1970.

[10] B. Roth, "Rigidity and flexible frameworks," *The American Mathematical Monthly*, vol. 88, pp. 6–21, January 1982.

[11] W. Whiteley and T. Tay, "Generating isostatic frameworks," *Structural Topology*, vol. 11, pp. 21–69, 1985.

[12] R. Olfati-Saber and R. Murray, "Graph rigidity and distributed formation stabilization of multi-vehicle systems," in *Proceedings of the IEEE Conference on Decision and Control*, 2002.

[13] T. Eren, P. Belhumeur, B. Anderson, and A. Morse, "A framework for maintaining formations based on rigidity," in *Proceedings of the IFAC Congress*, 2002, pp. 2752–2757.

[14] P. S. Maybeck, *Stochastic Models, Estimation and Control*. Academic Press, 1979.